Electronic Supplementary Material (ESI) for Nanoscale.

Supporting Information

Frequency-selective electrokinetic enrichment of biomolecules in physiological media based on electrical double-layer polarization

Ali Rohani[a], Bankim J. Sanghavi[a], Armita Salahi[a], Kuo-Tang Liao[b], Chia-Fu Chou[b], Nathan S. Swami[a]*

a – Department of Electrical & Computer Engineering, University of Virginia, Charlottesville, Virginia-22904, USA

b – Institute of Physics, Academia Sinica, Taipei-11529, Taiwan

* Corresponding Author. Fax: +1-434-924-8818.

Email: nswami@virginia.edu

S1. Experimental device geometry and operation:

The overall device geometry is shown in Figure S1 [S1]. As per the cross-section view in Figure S1c, and top view in Figure S1a, four reservoirs lead to a microchannel of 5 μm depth and a nanoslit with 200 nm depth, 30 μm width and 300 μm length. As per Figure S1c, a sharp lateral constriction down to a constriction gap of ~40 nm is used to create the surface charge non-uniformity. All experiments were conducted in a supporting electrolyte of phosphate buffer saline (PBS; 0.1 M, pH 6.5) of ~1.6 S/m conductivity. Terminals 1 and 3 are tied together and terminals 2 and 4 are tied, so that a 180-degree out of phase AC field (70 V_{rms}/cm at 1 MHz) can be applied offset by a 1.5 V_{DC}/cm field, with terminals 2 &4 forming the cathodic terminals. The data described herein is shown for the constriction within the red box of Figure S1b.

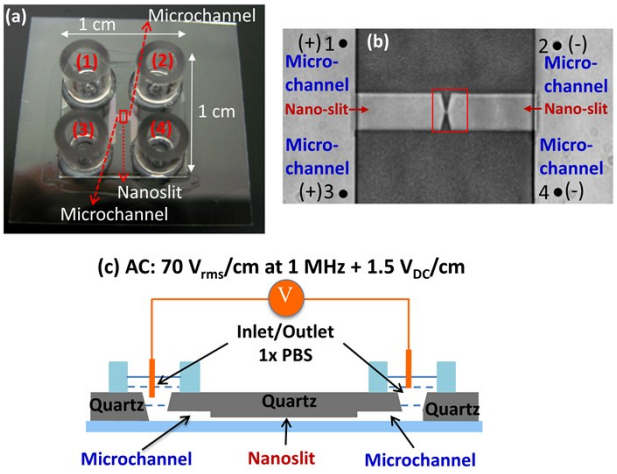

Figure S1: (a) Top view of overall device, (b) View of the nanoslit, and (c) Cross-section view.

S2: Dynamic ellipsoidal model of polarization dispersion for colloids

Sizes of the proteins are much smaller than the special non-uniformity of the electric field distribution within nano-channels, and consequently the overall shape of the protein is seen by the external field distribution. Multiple studies show that spheres or ellipsoids can approximate the overall shape of proteins [S2- S7]. These models have also been successfully used in different studies to validate the behavior of proteins [S8 – S11].

In this study we define a dynamic structure for the proteins, where the properties of the surrounding double layer actively changes in response to external electric field's frequency.

While the overall shape of the proteins is modeled through an ellipsoidal core with 3 degrees of freedom (axis along different directions), the effects of small structural differences within protein structures or on the surface are reflected in dielectric properties of core, and the active surrounding layer.

We use an ellipsoidal structure as the basis of our protein model to better capture the general asymmetry of the protein structure in different directions. Due to asymmetry, ellipsoidal particles experience different levels of polarizability in different directions under external electric field, which influences their behavior at different directions. This difference in polarizability manifests itself in a factor called depolarization factor A_i, where $i = x, y, z$. Depolarization factor is the ratio of the internal electric field induced by the charges on the surface of a dielectric under an external field to the net polarization of the dielectric. The following sum is valid for particles of various shapes.

$$A_x + A_y + A_z = 1 \ldots Eq.\ (S1)$$

For a sphere with omnidirectional symmetry, the depolarization factor is: 1/3, i.e. equal in all directions. The DEP force on ellipsoidal particles can be analytically found in a similar way to spherical particles by change of variables [S12]. The DEP force on a prolate spheroid oriented with its major axis (x: as denoted by subscript on $K_{x,0}$) along the electric field direction is given by:

$$F_{DEP} = 2\pi\varepsilon_m abc Re\left[K_{x,0}\ \right] \cdot \nabla(E.E) ... Eq.\ (S2)$$

Here: $a > b,\ c$ are axis lengths along x, y, and z directions, respectively; and: $K_{x,0}$, is the net complex spheroidal Clausius-Mossotti factor of particle with no shell (denoting subscript: "0") is defined as:

$$K_{x,0}\ (\omega) = \frac{1}{3}\left[\frac{{\varepsilon_p}^* - {\varepsilon_m}^*}{{\varepsilon_m}^* + A_x\left({\varepsilon_p}^* - {\varepsilon_m}^*\right)}\right] ... Eq.\ (S3)$$

A_x is depolarization factor along major axis (x), and is defined as:

$$A_x = \frac{1 - e^2}{2e^3}\left[\log\left(\frac{1+e}{1-e}\right) - 2e\right] ... Eq.\ (S4)$$

Here: $= \sqrt{1 - \frac{bc}{a^2}}$; is the particle eccentricity.

Next, we consider nanocolloidal biomolecules as composed of an insulating core with a net Clausius-Mossotti factor of: $K_{Core,x}$ and a conducting double-layer (subscript: *dl*) of thickness κ^{-1}. The term: $K_{Core,x}$ is formulated similar to $K_{x,0}$, but with the corresponding dielectric properties of the core versus the double-layer, whereas $K_{x,1}$, is the net complex Clausius-Mossotti factor of the spheroidal colloid with one shell (denoting the "1" in the subscript). These Clausius-Mossotti factor terms are analogous to $\tilde{f}_{CM}$ for spherical particles. The DEP behavior of this spheroidal single-shell core with a confocal shells to model the surrounding double layer is used to compute the complex spheroidal dipole coefficient along the major axis (x) as:

$$K_{x,1}(\omega) = \frac{1}{3}\left[\frac{({\varepsilon_{dl}}^* - {\varepsilon_m}^*) + 3K_{Core,x}\rho[{\varepsilon_{dl}}^* + A_{dl,x}({\varepsilon_m}^* - {\varepsilon_{dl}}^*)}{{\varepsilon_m}^* + A_{dl,x}\left({\varepsilon_{dl}}^* - {\varepsilon_m}^*\right) + 3K_{core,x}\rho\, A_{dl,x}(1 - A_{dl,x})\left({\varepsilon_{dl}}^* - {\varepsilon_m}^*\right)}\right] ... Eq.\ (S5)$$

$$K_{core,x}\ (\omega) = \frac{1}{3}\left[\frac{{\varepsilon_{core}}^* - {\varepsilon_{dl}}^*}{{\varepsilon_{dl}}^* + A_x\left({\varepsilon_{core}}^* - {\varepsilon_{dl}}^*\right)}\right] ... Eq.\ (S6)$$

Here: $A_{dl,x} = \frac{1 - e_{dl}^2}{2e_{dl}^3}\left[\log\left(\frac{1+e_{dl}}{1-e_{dl}}\right) - 2e_{dl}\right]$ is the depolarization factor of the biomarker and its surrounding double layer, with eccentricity defined as $e_{dl} = \sqrt{1 - \frac{(b + \kappa^{-1})(c + \kappa^{-1})}{(a + \kappa^{-1})^2}}$. The volume ratio (ρ) is:

$$\rho_{dl} = \frac{a.b.c}{(a + \kappa^{-1}) \cdot (b + \kappa^{-1}).(c + \kappa^{-1})} ... Eq.\ (S7)$$

Based on this, the dispersion of $K_{x,1}$ is computed for an ellipsoid (major to minor axis of 4:1) versus a sphere. The diameter of the sphere is the same as the major axis of the ellipsoid.

While an ellipsoidal model was developed to model the overall structure of the protein and capture its overall asymmetry, the surface properties and miniature structural variations in the protein structure are captured through the dynamic surrounding layer in our ellipsoidal model.

The basis of the dynamic surrounding layer in our model is Schwarz model of diffused double layer polarization, where ions can move freely in the double layer around the particle surface [S13], but cannot leave the double-layer. Based on this model the current density in our surrounding layer has two components; (1) flux of ions at the surface; and (2) diffusion flux acting against it. Derived current density in this model can be used to find the charge density perturbation at the interface, which in turn can be used to find the potential around the particle. Solving these equations will result in a frequency dependent surface conductance:

$$K_s = \left(\frac{2k_s}{a}\right)\left(1 + \frac{i\omega\tau}{1 + i\omega\tau}\right) \ldots Eq.\ (S8)$$

Based on this, the complex permittivity of the double layer can be defined as:

$$\varepsilon^* = \left(\frac{2k_s}{a}\right)\left(\frac{\tau}{1 + \omega^2\tau^2}\right) - i\left(\left(\frac{2k_s}{a}\right)\left(1 + \frac{\omega\tau}{1 + \omega^2\tau^2}\right)\right) \ldots Eq.\ (S9)$$

To a good approximation, we can consider epsilon of the double layer to be invariant with frequency for < 10 MHz range. The frequency dependent conductivity of double layer can be defined as [S14]:

$$\sigma_{dl} = \left(\frac{2k_s}{a}\right)\left(1 + \frac{\omega^2\tau}{1 + \omega^2\tau^2}\right) \ldots Eq.\ (S10)$$

Here, dynamic behavior of the double-layer conductivity versus frequency is determined by a time constant defined as the following [S14]:

$$\tau = \frac{2\pi\left(a + \kappa^{-1}\right)^2}{D} \ldots Eq.\ (S11)$$

D is diffusion coefficient and κ^{-1} (or: λ) is ionic strength-dependent thickness of electrical double-layer. These equations are used to compute the dispersions plotted in Figure 3 and Figure 4 of the manuscript.

All simulation parameters are similar to those used for Figure 3. It is apparent from Figure S2 that an ellipsoidal shape causes higher pDEP levels and widens the pDEP magnitude, as explained within the manuscript.

Based on this, the dispersion of $K_{x,1}$ is computed for an ellipsoid (major to minor axis of 4:1) versus a sphere. The diameter of the sphere is the same as the major axis of the ellipsoid. All other simulation parameters are similar to those used for Figure 3. It is apparent from Figure S2 that an ellipsoidal shape causes higher pDEP levels and widens the pDEP magnitude, as explained within the manuscript.

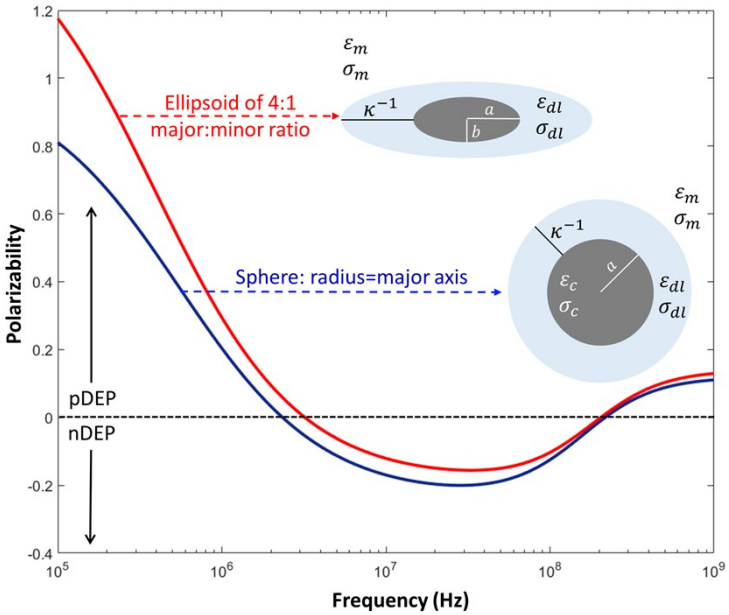

Figure S2: Simulated dispersion of ellipsoidal versus spherical particles with equivalent major axes. Simulation parameters are the same as in Figure 3.

References

[S1] Sanghavi, B. J.; Varhue, W.; Rohani, A.; Liao, K.-T.; Bazydlo, L. A. L.; Chou, C.-F.; Swami, N. S., Ultrafast immunoassays by coupling dielectrophoretic biomarker enrichment in nanoslit channel with electrochemical detection on graphene. Lab Chip 2015, 15, 4563-4570.

[S2] Chapman, Tara L., et al. "Crystal structure and ligand binding properties of the D1D2 region of the inhibitory receptor LIR-1 (ILT2)." *Immunity* 13.5 (2000): 727-736.

[S3] Devedjiev, Yancho, et al. "The structure and ligand binding properties of the B. subtilis YkoF gene product, a member of a novel family of thiamin/HMP-binding proteins." *Journal of molecular biology* 343.2 (2004): 395-406.

[S4] Kragh-Hansen, Ulrich. "Structure and ligand binding properties of human serum albumin." *Danish medical bulletin* 37.1 (1990): 57-84.

[S5] Sandin, Sara, et al. "Structure and flexibility of individual immunoglobulin G molecules in solution." *Structure* 12.3 (2004): 409-415.

[S6] Grant, E. H., G. P. South, and I. O. Walker. "The dipole moment of myoglobin." *Biochemical Journal* 122.5 (1971): 765.

[S7] Jacobson, R. H., et al. "Three-dimensional structure of β-galactosidase from E. coli." *Nature* 369.6483 (1994): 761-766.

[S8] Mohamad, Ahmad Sabry, et al. "A dielectrophoresis-impedance method for protein detection and analysis." *AIP Advances* 7.1 (2017): 015202.

[S9] Zheng, Lifeng, Peter J. Burke, and James P. Brody. "Electronic manipulation of DNA and proteins for potential nano-bio circuit assembly." *Proc. of SPIE Vol*. Vol. 5331. 2004.

[S10] Gunda, Naga Siva Kumar, and Sushanta Kumar Mitra. "Modeling of dielectrophoretic transport of myoglobin molecules in microchannels." *Biomicrofluidics* 4.1 (2010): 014105.

[S11] Clarke, Richard W., et al. "Surface conductivity of biological macromolecules measured by nanopipette dielectrophoresis." *Physical review letters* 98.19 (2007): 198102.

[S12] Fernandez, Renny E., et al. "Microbial analysis in dielectrophoretic microfluidic systems." *Analytica Chimica Acta* (2017).

[S13] Schwarz: A theory of the low-frequency dielectric dispersion of colloidal particles in electrolyte solution J. Phys. Chem. 66 2636-2642 (1962)

[S14] Morgan, H.; Green, N. G., AC electrokinetics: colloids and nanoparticles. Research Studies Press; Institute of Physics Pub.; Distribution, North America, AIDC: Baldock, Hertfordshire, England; Philadelphia, Pa.; Williston, VT, 2003; p xvi, 324 p